

Georgia Journal of Science

Volume 77 No. 2 *Scholarly Contributions from the Membership and Others*

Article 2

2019

Measurement of Solar Spectral Irradiance and Surface Ozone at Carrollton, Georgia, USA, During the Great American Eclipse on 21 August 2017

Kirthi Tennakone

Georgia State University, ktenna@yahoo.co.uk

L Ajith DeSilva

State University of West Georgia, ldesilva@westga.edu

Charles A. Zander*

University of West Georgia, Carrollton, GA 30118, czander1@my.westga.edu


Shea Rose

University of West Georgia, srose@westga.edu

Austin B. Kerlin

Follow this and additional works at: <https://digitalcommons.gaacademy.org/gjs>

University of West Georgia, akerlin2@gmail.com

 Part of the [Atmospheric Sciences Commons](#), [Atomic, Molecular and Optical Physics Commons](#), [Climate Commons](#), [Environmental Monitoring Commons](#), [Natural Resources and Conservation Commons](#), [Other Astrophysics and Astronomy Commons](#), and the [The Sun and the Solar System Commons](#)

Recommended Citation

Tennakone, Kirthi; DeSilva, L Ajith; Zander*, Charles A.; Rose, Shea; and Kerlin, Austin B. (2019) "Measurement of Solar Spectral Irradiance and Surface Ozone at Carrollton, Georgia, USA, During the Great American Eclipse on 21 August 2017," *Georgia Journal of Science*, Vol. 77, No. 2, Article 2.

Available at: <https://digitalcommons.gaacademy.org/gjs/vol77/iss2/2>

This Research Article is brought to you for free and open access by Digital Commons @ the Georgia Academy of Science. It has been accepted for inclusion in Georgia Journal of Science by an authorized editor of Digital Commons @ the Georgia Academy of Science.

Measurement of Solar Spectral Irradiance and Surface Ozone at Carrollton, Georgia, USA, During the Great American Eclipse on 21 August 2017

Acknowledgements

This research did not receive any specific grant from funding agencies in the public, commercial, or not-for-profit sectors.

MEASUREMENT OF SOLAR SPECTRAL IRRADIANCE AND SURFACE OZONE AT CARROLLTON, GEORGIA, USA, DURING THE GREAT AMERICAN ECLIPSE ON 21 AUGUST 2017

Kirthi Tennakone
Department of Physics and Astronomy,
Georgia State University, Atlanta, Georgia, 30303

L. Ajith DeSilva*
Department of Physics,
University of West Georgia, Carrollton, Georgia, 30118

Charles Zander
Department of Physics,
University of West Georgia, Carrollton, Georgia, 30118

Shea Rose
Department of Geosciences,
University of West Georgia, Carrollton, Georgia, 30118

Austin Kerlin
Department of Physics,
University of West Georgia, Carrollton, Georgia, 30118

*corresponding author: ldesilva@westga.edu

ABSTRACT

Measurements conducted at the University of West Georgia, Carrollton, Georgia, during the time of the solar eclipse of 21 August 2017, demonstrated that the integrated spectral irradiance in defined wavelength ranges in the ultraviolet and visible calculated as a fraction of the total irradiance reached a minimum at maximum obscuration of the Sun, whereas in the infrared range it was maximum. The method of analysis adopted supports the view that the changes in spectral irradiance during highly obscured partial phases is a consequence of limb darkening. In a surface ozone measurement, the minimum ozone concentration occurred 30 ± 5 min after the instant of maximum obscuration. This observation is explained as a combined effect of a change in reaction rates of photochemical generation and degradation of ozone.

Keywords: solar eclipse; spectral irradiance; surface ozone; photochemical reactions; limb darkening

INTRODUCTION

It is well known that during a solar eclipse the light intensity variation accompanies a change in spectral irradiance. The light intensity changes far more rapidly during the progress of a solar eclipse, compared to the diurnal pattern, and induces distinct physical and photochemical atmospheric effects. Recently, Ilić et al. (2018) reported measurements of meteorological parameters, solar radiation, surface ozone air ionization, and low frequency electromagnetic signals originating from plasma oscillations during the eclipse of 15 March 2015. Changes in column (Chakrabarty et al. 1997; Manchanda et

al. 2012) and surface (Tzanis et al. 2008; Zanis et al. 2007) ozone have been observed, as the phase of the eclipse passed the point of maximum obscuration. Miscellaneous effects of solar eclipses on the atmosphere and biosphere have also been studied by several authors (Gerasopoulos et al. 2008; Paramitha et al. 2017; Ahrens et al. 2001; Thampi et al. 2010).

There are many records of solar irradiance measurements (Antón et al. 2005; Kazantzidis et al. 2007; Tzanis et al. 2008; Blumthaler et al. 2006) conducted during the time of solar eclipses and simulations representing those effects (Emde and Mayer 2007). Generally, spectral irradiance changes during an eclipse are attributed to limb darkening (Hestroffer and Magnan 1998; Kazadzis et al. 2007; Kazantzidis et al. 2007; Koepke 2001). Limb darkening (Neckel 1996; Neckel and Labs 1994; Hestroffer and Magnan 1998; Raponi et al. 2012) or intensity variation across the solar disc is wavelength dependent as optical depth varies with this parameter. Kazadzis et al. (2007) discussed the spectral effect of limb darkening in global, direct irradiance and actinic flux measurements that leads to a more pronounced decrease in radiation at the lower wavelengths. The above findings have been verified by Kazantzidis et al. (2007) who measured global horizontal UV. Further, the observation was supported by photosynthetically active radiation model calculations. Modelling of the extraterrestrial solar flux to simulate the conditions of an eclipse and comparison with measurements have also revealed that spectral irradiance at specific wavelengths is significantly altered by limb darkening (Koepke et al. 2009).

Although measurements of solar irradiance and physical and photochemical effects due to photon flux variation during different solar eclipses are grossly similar, significant qualitative as well as quantitative differences dependent on the degree of obscuration, zenith angle, and geographical location of the observation site have been noted. Obviously, in a set of such measurements, it is highly improbable that several measurements correspond to identical conditions. As there are too many variables (astronomical parameters of the eclipse, weather, and other atmospheric conditions), even two measurements' conditions would never be identical. Thus, each measurement has its own value for comparison and archival records. Furthermore, almost all studies interpreting spectral irradiance variations during solar eclipses as a result of limb darkening are confined to specific wavelengths. For comparison of different measurements, and explaining the unusual color in twilight, like dimming of sunlight during a solar eclipse when the obscuration is large, it is desirable to compute relative spectral irradiance in broader ranges of wavelengths in infrared, visible, and ultraviolet. An advantage of this method is smoothing of errors due to the presence of Fraunhofer absorption lines. The present work describes measurements of total global irradiance, spectral irradiance, and surface ozone at the University of West Georgia, Carrollton, Georgia, United States, during the time of the solar eclipse of 21 August 2017, where the maximum obscuration was ~95%. The spectral irradiance data were analyzed using a novel method of computing the time-variation of the integrated irradiance in the following wavelength ranges: infrared (701–1040 nm), visible (391–700 nm), and ultraviolet (300–390 nm). This procedure more convincingly demonstrates that the observed spectral changes are mainly related to the phenomenon of limb darkening.

THE EXPERIMENT

Local Conditions and Measurements

Carrollton is a typical urban city in the southern United States, of geographical coordinates 33.5801 N, 85.0766 W, and elevation of 336 m. Measurements were carried out in a dust free rooftop 12 m above ground level at the University of West Georgia, Carrollton. The observation site was not interrupted by shadows of buildings or trees. Monitoring conducted days before the eclipse convinced us that, at the Sun’s position in the sky during the time of the eclipse, there would not be significant external ground level environmental factors such as moving vehicles or reflecting objects affecting time variation solar flux. On 21 August 2017, the visibility at the site was 16 km, with a moderate air quality index of 55. During the time of measurement, the sky was clear except for scattered thin clouds that developed ~30 min after the first contact and lasted until ~15 min before the maximum obscuration. Humidity and temperature varied in the ranges of 93–96% and 29–30 °C. Air pressure remained at ~1 atm, and no significant wind was reported (Weather Aug. 17, 2017).

A LabQuest Vernier pyranometer (sensitive to the wavelength range 370–1140 nm) recorded the global total horizontal solar irradiance with a 180° field of view angle and an Ocean Optics QE 64 spectrometer (298–1080 nm) with a cosine corrector (Kerlin et al. 2016) was used to monitor the global horizontal spectral irradiance by recording two sets of readings every minute. The cosine corrector and spectrometer were coupled with a 50 µm fiber to a computer to record the data. The setup was calibrated using an Ocean Optics HL-2000-cal tungsten-halogen lamp. The ambient surface ozone concentration was monitored with a calibrated Aeroqual S500 ozone detector equipped with a semiconductor (tungsten oxide) gas sensor head (Kanda 2015), which closed direct sunlight entry, and allowed free air passage. For comparison and rehearsal, all experiments were also conducted on the day previous to the eclipse and around same time period (1:00–4:30 pm).

The Eclipse at Carrollton, Georgia, USA

The altitude and azimuth of the Sun at the time of the start, maximum, and end of the eclipse in Carrollton obtained from NASA’s Eclipse website are shown Table I. The maximum magnitude drop and the percentage obscuration at this location were 0.95776 and 95.4091 respectively.

Table I. Altitude and azimuth at the time of the start, maximum, and end of the partial eclipse in Carrollton on 2017 Aug. 21. Data were taken from the NASA Eclipse website (NASA website 2017).

Event	Local Time (Eastern Time)	Attitude	Azimuth
Start of the partial eclipse	1:04:25.5 pm	+65.5°	155.4°
Maximum eclipse	2:35:31.1 pm	65.2°	211.8°
End of the partial eclipse	4:01:03.2 pm	+51.8°	243.5°

RESULTS AND DISCUSSION

The variation of global irradiance measured with the pyrometer is shown in Figure 1. The broken-line curve in Figure 1 shows a simulation of the percentage of uncovered Sun (NASA website 2017). The coincidence of the minimum of this curve with minimum of irradiance demonstrates that the scattered thin clouds, which developed 30 min after the eclipse and lasted until 15 min before the maximum obscuration, had no effect. The observed nonsymmetry between variations of irradiance and the percentage uncovered area of the Sun in Figure 1 is due to a combination of eclipse effect and zenith angle related to irradiance changes.

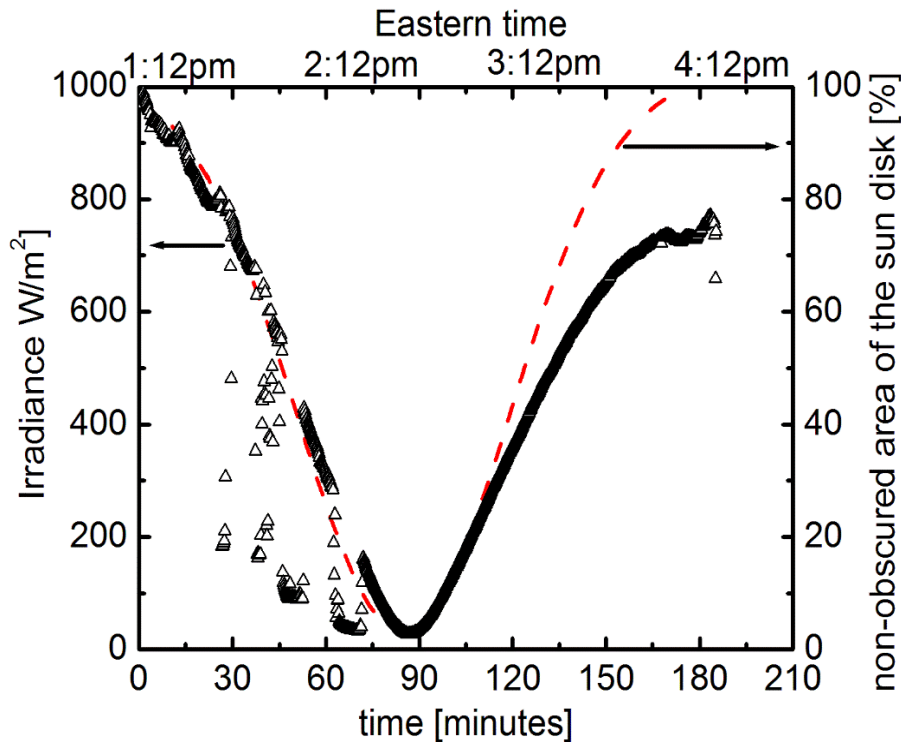


Figure 1. Variation of global irradiance with time measured with a pyrometer sensitive to the wavelength range 370–1140 nm. The scattered data points seen 30–75 min from the start of the eclipse are a result of a thin cloud cover that developed during that period. The broken-line curve is a simulation of the percentage of the uncovered area of the Sun. Triangle data points and the broken-line curve refer to left and right vertical axes, respectively, as indicated by arrows.

With data extracted from the measurements, a series of plots of $I(\lambda, t)$ (= spectral irradiance at wavelength λ measured at time t) vs λ , were analyzed by the following procedure. The ratio $R(\lambda_2, \lambda_1, t)$ is defined by the expression,

$$R(\lambda_2, \lambda_1, t) = \frac{\int_{\lambda_1}^{\lambda_2} I(\lambda, t) d\lambda}{\int_{\text{Entire range of } \lambda} I(\lambda, t) d\lambda} \tag{1}$$

which measures the total irradiance in the wavelength range λ_2 to λ_1 at time t as a fraction of the total intensity. The quantity $R(\lambda_2, \lambda_1, t)$ is calculated for the wavelength ranges; (300–390 nm), (391 – 700 nm), and (701 – 1040 nm); corresponding to ultraviolet (UV), visible (Vis), and infrared (IR) regions of the spectrum. The time variation of percentages of these ratios are plotted in Figure 2 (a). To compare the R values before first contact, Figure 2(b) plots of R are normalized to the values of the respective ratios before the eclipse (i.e., $R(t) \%$ is divided by $R(t = 0)$ for IR, Vis, and UV). This plot displays the change in spectral irradiance due to the eclipse more conspicuously. The plot of Figure 2 (b) confirms that limb darkening attenuates UV more strongly compared to longer wavelengths. Zerefos et al. (2000, 2001) observed at the time of maximum obscuration (88%) of the eclipse of August 1, 1999, at Thessaloniki in Greece, that UV radiation in a similar range (285–365 nm) is most strongly attenuated, and the effect is attributed to limb darkening.

Clearly, the percentage of ultraviolet and visible has dropped at the maximum of the eclipse with an increase in the percentage of infrared. The change in spectral irradiance sunlight during a solar eclipse is attributed mainly to limb darkening—the

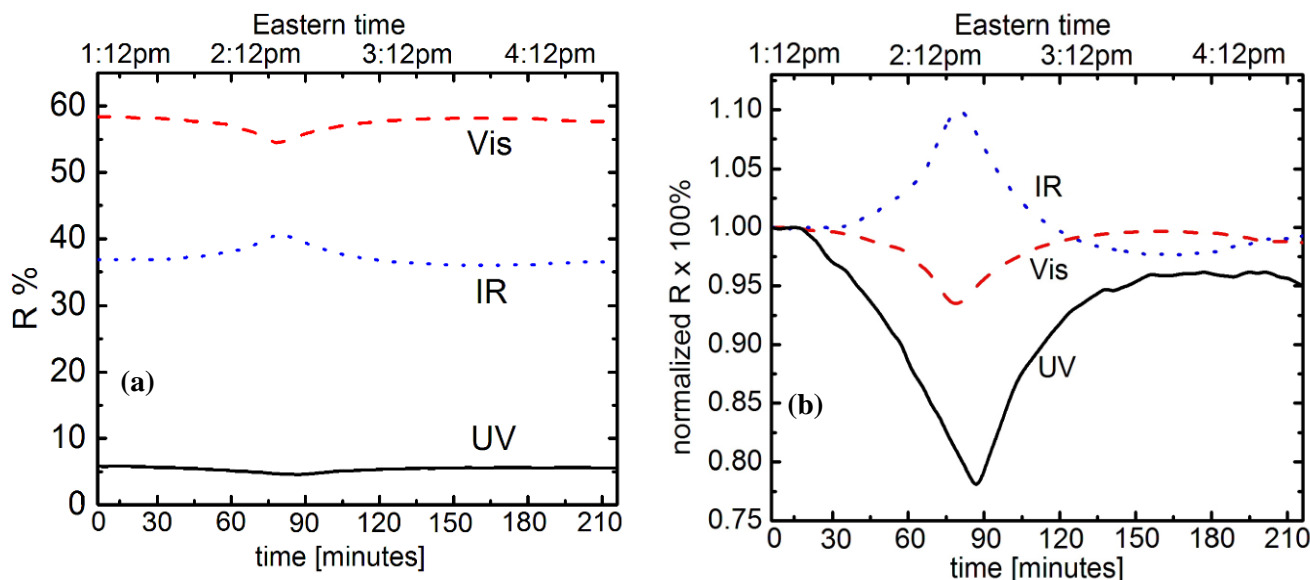


Figure 2. (a) The ratio R (expressed as a percentage) defined by equation (1) for the ultraviolet-UV (300–390 nm), visible-Vis (391–700 nm), and infrared-IR (701–1040 nm) wavelength ranges of the spectrum. (b) Normalized R to pre-eclipse ratios of UV, Vis, and IR.

brightness and spectral radiance distribution over the solar disc, which is more pronounced at shorter wavelengths towards blue end of the spectrum and less pronounced in the far red (Rubin 1959; Hestroffer and Magnan 1998; Kazadzis et al. 2007; Kazantzidis et al. 2007; Koepke 2001). The method used here in analyzing the time variation of spectral irradiance reveals this effect conspicuously. Multiple scattering of light could also induce spectral changes noticeable during the total phase (Kazadzis et al. 2007; Kazantzidis et al. 2007). This effect is noticeable only at low illuminations during totality, is insignificant even at large obscurations, and the pattern variation seen cannot be accounted by multiple scattering.

The time variation of the surface ozone concentration at the measurement site is presented in Figure 3 (a) and, for comparison, the results of the same measurement conducted the previous day around the same time are shown in Figure 3 (b). The dashed-line curve in Figure 3 (a) indicates the variation of the nonobscured area of the solar disk. During the eclipse, surface ozone concentration had decreased from ~ 0.10 ppm to a minimum of ~ 0.07 ppm 30 min after the maximum obscuration.

Surface ozone is produced by oxidation of carbon monoxide, methane, and nonvolatile organic compounds in the presence of nitrogen dioxide, which acts as a photocatalyst by absorbing radiation wavelengths less than 420 nm (Tzanis et al. 2008; Zanis et al. 2007). Air pollution, notably from traffic and industries, generates these ozone precursors and distributes them by diffusion and wind. Ozone is also transported from the stratosphere to the troposphere. However, in the relatively short duration of the eclipse, the change in ozone concentration due to this process cannot be significant. Consequently, a change in surface ozone during a solar eclipse reflects more clearly the local production and destruction of ozone. As diffusion is negligible, the rate of change of the ozone concentration can be written as,

$$\frac{d}{dt}[O_3] = aI(t) - k[O_3] - hI(t)[O_3] \quad (2)$$

where $I(t)$ = light intensity in the photochemically active wavelengths, $[O_3]$ = ozone concentration, and a , k and h are constants independent of light intensity but dependent on other factors such as air pollutant concentrations. Some atmospheric pollutants and nitrous oxide (an intermediate of the photocatalytic ozone production step) also act as agents destroying ozone directly and via photochemical reactions. The first term in RHS (2) accounts for photochemical production of ozone, and the second and third terms represent direct and photochemical degradation of ozone.

The extremal of $[O_3]$ corresponds to the condition,

$$aI(t) - k[O_3] - hI(t)[O_3] = 0. \quad (3)$$

Using (2) and (3), the second derivative (2) at the extremum of $[O_3]$ can be expressed as,

$$\frac{d^2}{dt^2}[O_3] = ak[k + hI(t)]^{-1} \left[\frac{dI(t)}{dt} \right]. \quad (4)$$

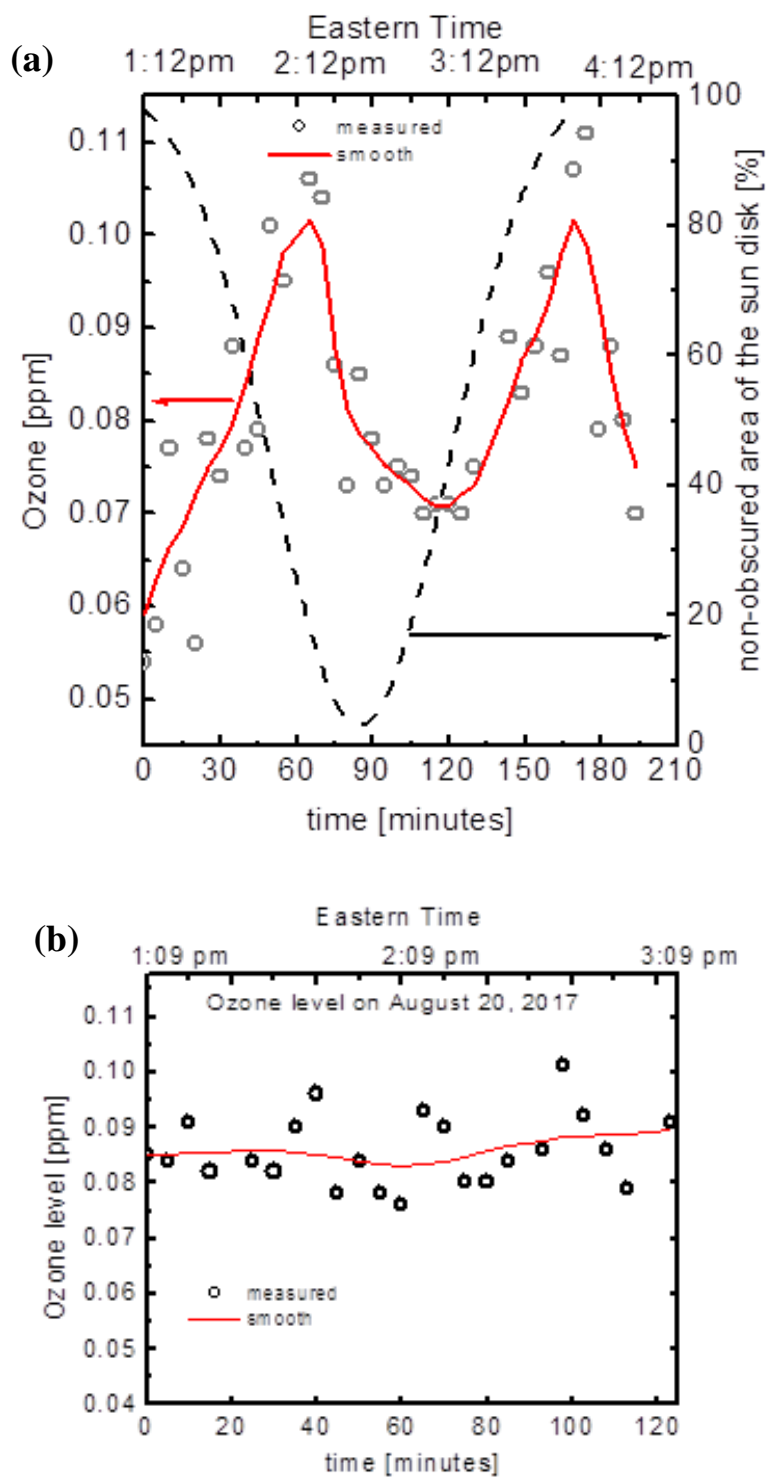


Figure 3. Time variation of the surface ozone concentration at the measurement site. Data circles (left vertical axis) and dashed-lines (right vertical axis) are indicated by arrows and, for comparison, the results of the same measurement conducted the previous day around the same time are shown in Figure 3 (b). A 5-point fast Fourier transform data smoothing was done to reduce the noise, and the smoothened curve is marked red.

From (4), it follows that the extremum turns out to be a minimum, provided $\frac{dI(t)}{dt} > 0$. Thus, it is clear from Figure 3 (a) the minimum of $[O_3]$ should occur after the minimum of the light intensity. It is interesting to note that the minimum of UV in Figure 2 (a) occurs slightly after the Vis and IR peaks, and this indication is seen to be more pronounced in Figure 2 (b). Column ozone attenuates UV and, as creation and destruction of ozone depends on light intensity, the peak gets shifted—an effect similar to the case of surface ozone.

CONCLUSIONS

Measurements conducted at Carrolton, West Georgia, at the time of the solar eclipse of 21st August 2017, where the maximum obscuration was ~95%, revealed that there are changes in the spectral irradiance peak at the time of maximum obscuration. Ultraviolet (integrated irradiance in the wavelength range 300–390 nm) and visible (integrated irradiance in the wavelength range 391–700 nm) reached a minimum at this point, whereas in the infrared (integrated irradiance in the wavelength range 701–1040 nm) it was maximum. The fractional integrated irradiances normalized to pre-eclipse values in the UV and Vis ranges had decreased by 15 and 5%, respectively, whereas in the IR range there was an increase of 10%. The method of analysis presented strongly supports the view that the spectral changes during eclipse are mainly due to limb darkening. This analysis also masks errors in limb darkening measurements (Raponi et al. 2012) occurring due to nonmonotonic spectral profile of Fraunhofer lines.

The surface ozone measurement indicated a minimum concentration 30 ± 5 min after the time of maximum obscuration. The effect was explained as a result of the kinetics of photochemical generation of ozone and its degradation.

REFERENCES

- Ahrens, D., M.G. Iziomon, L. Jaeger, A. Matzarakis, and H. Mayer. 2001. Impacts of the solar eclipse of 11 August 1999 routinely recorded meteorological and air quality data in south-west Germany. *Meteorol., Z.* 10, 215–223. doi:[10.1127/0941-2948/2001/0010-0215](https://doi.org/10.1127/0941-2948/2001/0010-0215).
- Antón, M., A. Serrano, M. Cancillo, J. Vaquero, and J. Vilaplana. 2005. Solar irradiance and total ozone over El Arenosillo (Spain) during the solar eclipse of 3 October 2005. *J. Atmospheric Sol.-Terr. Phys.*, 72, 789–793. doi:[10.1016/j.jastp.2010.03.025](https://doi.org/10.1016/j.jastp.2010.03.025).
- Blumthaler, M., A. Bais, A. Webb, S. Kazadzis, R. Kift, R.N. Kouremeti, B. Schallhart, et al. 2006. Variations of solar radiation at the Earth's surface during the total solar eclipse of 29 March 2006. *Int. Soc. Opt. Eng.*, 63620F1-8. doi:[10.1117/12.689630](https://doi.org/10.1117/12.689630).
- Chakrabarty, D.K., N.C. Shah, and K.V. Pandya. 1997. Fluctuation in ozone column over Ahmedabad during the solar eclipse of 24 October 1995. *Geophys. Res. Lett.*, 24, 3001–3003. doi:[10.1029/97GL03016](https://doi.org/10.1029/97GL03016).
- Emde, C. and B. Mayer. 2007. Simulation of solar radiation during a total eclipse: A challenge for radiative transfer. *Chem. Phys.*, 7, 2259–2270. doi:[10.5194/acp-7-2259-2007](https://doi.org/10.5194/acp-7-2259-2007).
- Gerasopoulos, E., C.S. Zerefos, I. Tsagouri, D. Founda, V. Amiridis, A.F. Bais, A. Belehaki, et al. 2008. The total solar eclipse of March 2006: Overview. *Atmos. Chem. Phys.*, 8, 5205–5220. doi:[10.5194/acp-8-5205-2008](https://doi.org/10.5194/acp-8-5205-2008).

- Hestroffer, D. and C. Magnan. 1998. Wavelength dependency of the solar limb darkening. *Astron. Astrophys.*, 333, 338–342. <http://adsabs.harvard.edu/full/1998A%26A...333..338H>.
- Ilić, L., M. Kuzmanoski, P. Kolarž, A. Nina, V. Srećković, Z. Mijić, J. Bajčetić, et al. 2018. Changes of atmospheric properties over Belgrade, observed using remote sensing and in situ methods during the partial solar eclipse of 20 March 2015. *Atmospheric Sol.-Terr. Phys.*, 171, 250–259. doi:[/10.1016/j.jastp.2017.10.001](https://doi.org/10.1016/j.jastp.2017.10.001).
- Kanda, I. 2015. Measurement of ozone concentration on the elevation gradient of a low hill by a semiconductor-based portable monitor. *Atmosphere*, 6, 928–941. doi:[/10.3390/atmos6070928](https://doi.org/10.3390/atmos6070928).
- Kazadzis, S., A. Bais, M. Blumthaler, A. Webb, N. Kouremeti, R. Kift, B. Schallhart, et al. 2007. Effects of total solar eclipse of 29 March 2006 on surface radiation. *Atmos. Chem. Phys.*, 7, 5775–5783. doi:[/10.5194/acp-7-5775-2007](https://doi.org/10.5194/acp-7-5775-2007).
- Kazantzidis, A., A.F. Bais, C. Emde, S. Kazadzis, and C.S. Zerefos. 2007. Attenuation of global ultraviolet and visible irradiance over Greece during the total solar eclipse of 29 March 2006. *Atmos. Chem. Phys.*, 5959–5969. doi:[/10.5194/acp-7-5959-2007](https://doi.org/10.5194/acp-7-5959-2007).
- Kerlin, A.B., L.A. DeSilva, S. Rose, and J.E. Hasbun. 2016. Calculating the Sun's photospheric temperature, an undergraduate physics laboratory. *GA J. Sci.*, 74, article 13. <https://digitalcommons.gaacademy.org/gjs/vol74/iss2/13>.
- Koepke, P., J. Reuder, and J. Schween. 2001. Spectral variation of the solar radiation during an eclipse. *Meteorol. Z.*, 10, 179–186. doi:[/10.1127/0941-2948/2001/0010-0179](https://doi.org/10.1127/0941-2948/2001/0010-0179).
- Manchanda, R., P. Sinha, S. Sreenivasan, D. Trivedi, B. Kapardhi, B. Suneel Kumar, P.R. Kumar, et al. 2012. In-situ measurements of vertical structure of ozone during the solar eclipse of 15 January 2010. *Atmospheric Sol.-Terr. Phys.*, 84, 88–100. doi:[/10.1016/j.jastp.2012.05.011](https://doi.org/10.1016/j.jastp.2012.05.011).
- NASA website: 2017, Solar eclipse website USA. <https://eclipse.gsfc.nasa.gov/solar.html> (accessed 01 November 2017).
- Neckel, H. 1996. On the wavelength dependency of solar limb darkening ($\lambda 303$ to 1099 nm). *Sol. Phys.*, 167, 9–23. doi:[/10.1007/BF00146325](https://doi.org/10.1007/BF00146325).
- Neckel, H. and D. Labs. 1994. Solar limb darkening 1986–1990 ($\lambda 303$ to 1099 nm). *Sol. Phys.*, 153, 91–144. doi:[/10.1007/BF00712494](https://doi.org/10.1007/BF00712494).
- Paramitha, R., R. Zaen, and A. Nandiayanto. 2017. Changes in meteorological parameters (i.e. UV and solar radiation, air temperature, humidity and wind condition) during the partial solar eclipse of 9 March 2016. *IOC Conf. Ser.: Mater. Sci. Eng.*, 180, 012131.
- Raponi, A., C. Sigismondi, K. Guhl, R. Nugent, and A. Tegtmeier. 2012. Solar limb darkening function and solar diameter with eclipse observations. *Understanding solar activity: Advances and challenges*. EAS Publications Series, Edited by M. Faurobert, C. Fang, and T. Corbard, 55, 389–391. doi:[/10.1051/eas/1255056](https://doi.org/10.1051/eas/1255056).
- Rubin, V.C. 1959. Solar limb darkening determined from eclipse observations. *Astrophys. J.*, 129, 812–825. doi:[/10.1086/146677](https://doi.org/10.1086/146677).
- Thampi, A., M. Yamamoto, H. Liu, S. Saito, Y. Otsuka, and A. Patra. 2010. Nighttime-like quasi periodic echoes induced by a partial solar eclipse. *Geophys. Res. Lett.*, 37, L09107. doi:[/10.1029/2010GL042855](https://doi.org/10.1029/2010GL042855).

- Tzanis, C., C. Varotsos, and L. Viras. 2008. Impacts of the solar eclipse of 29 March 2006 on the surface ozone concentration, the solar ultraviolet radiation and the meteorological parameters at Athens, Greece. *Atmos. Chem. Phys.*, 425–430. doi:[/10.5194/acp-8-425-2008](https://doi.org/10.5194/acp-8-425-2008).
- Weather, Aug. 17, 2017: website <https://www.wunderground.com/> zip code 30118. (accessed 27 August 2017).
- Zanis, P., E. Katragkou, M. Kanakidou, B.E. Psiloglou, S. Karathanasis, M. Vrekoussis, E. Gerasopoulos, et al. 2007. Effects on surface atmospheric photo-oxidants over Greece during the total solar eclipse event of 29 March 2006. *Atmos. Chem. Phys.*, 7, 6061–6073. doi:[/10.5194/acp-7-6061-2007](https://doi.org/10.5194/acp-7-6061-2007).
- Zerefos, C.S., D.S. Balis, C. Meleti, A.F. Bais, K. Tourpali, K. Kourtidis, K. Vanicek, et al. 2000. Changes in surface solar UV irradiances and total ozone during the solar eclipse of August 11, 1999. *J. Geophys. Res.*, 105, 26463–26473. doi:[/10.1029/2000JD900412](https://doi.org/10.1029/2000JD900412).
- Zerefos, C.S., D.S. Balis, P. Zanis, C. Meletir, A.F. Bais, K. Tourpali, D. Melis, et al. 2001. Changes in surface UV solar irradiance and ozone over the Balkans during the eclipse of August 11, 1999. *Adv. Space Res.*, 27, 1955–1963. doi:[/10.1016/S0273-1177\(01\)00279-4](https://doi.org/10.1016/S0273-1177(01)00279-4).